

Tests of two-boson approaches for $^{16}\text{O}^\dagger$

F. Darema-Rogers* and William W. True

Physics Department, University of California, Davis, California 95616

(Received 21 March 1978)

The approximations of the interacting boson approximation of Iachello and Feshbach and the ability of this approach to describe the ^{16}O nucleus are tested. In the interacting boson approximation some "exchange" parts of many-boson matrix elements and violation of the Pauli principle in many-boson states are ignored. Matrix elements, two-boson wave functions and energies resulting from the interacting boson approximation are compared with exact two-hole two-particle calculations for the lowest 2^+ , 0^+ and the lowest excited 0^+ , 0^- states in ^{16}O . It was found that neither of the above two approximations of the interacting boson approximation are valid. Calculations without these two approximations improve the approximate energies but not the wave functions.

[NUCLEAR STRUCTURE ^{16}O ; calculated structure of lowest 0^+ and 2^+ excited levels. Interacting boson and shell model approaches.]

I. INTRODUCTION

Shell model calculations are fairly successful in explaining many features of the low lying states in spherical nuclei near doubly magic numbers. For such nuclei one considers only a few particles outside a doubly magic core, or a few holes in a doubly magic core, or a few holes in and a few particles outside a doubly magic core, and tries to choose as a basis those configurations which will be important in describing the structure of the low lying states. It is necessary that a truncated basis be used in order that the matrices that are diagonalized are of a finite size. Typical examples of such shell model calculations are given in Refs. 1-5.

When one tries to extend these shell model calculations away from closed shells to include many holes and/or particles, the number of basis configurations rapidly become too large to handle. In such cases several methods are commonly used to limit the size of the matrix to be diagonalized. One method is to severely truncate the number of basis states allowed. Only limited success has been obtained this way because important configurations have often not been included due to truncation. Another method⁶⁻⁸ is to do a "two-step" calculation. In this approach, one first calculates the energy spectrum of one or two nuclei which have only a few valence particles and then forms a truncated basis for a more complex nucleus by constructing product wave functions from a few of the low lying states obtained in the first step of the calculation. For example, several low lying levels in ^{206}Pb and ^{210}Po were coupled together to form a basis for ^{208}Po shell model calculations.⁸ An approach similar to the two-step approach de-

scribed above was proposed by Iachello⁹ and by Feshbach and Iachello¹⁰ (FI), which they called the interacting boson approximation (IBA).

This paper will explore and discuss the validity of the approximations made in the IBA model^{9,10} as applied to the ^{16}O nucleus. In Sec. II, the necessary formalism is developed. Section III discusses the boson basis used. Section IV will discuss the IBA results for ^{16}O , while Sec. V will examine what happens when some of the approximations made in the IBA model are removed. Section VI will compare the results of Secs. IV and V with a more complete calculation.

II. FORMALISM

In this section, the formulas and terminology will be given which will help one to understand the approach and approximations made in the IBA model used by Feshbach and Iachello^{9,10} and the calculations presented in this paper.

A. Shell model Hamiltonian

The shell model Hamiltonian will be written schematically as

$$H = H_C + H_{pC} + H_{hC} + H_{hp} + H_{pp} + H_{hh} + H'. \quad (1)$$

H_C represents the ^{16}O closed core energy, and all energies used will be relative to this core energy causing H_C to have an expectation value of zero for any state considered. Consequently, H_C will be ignored from now on. H_{pC} describes the kinetic energy of a particle in an orbital outside the ^{16}O core and its interaction with the core particles. H_{hC} similarly describes the kinetic energy and interaction energy of a hole in an orbital in the core.

H_{hp} , H_{pp} , and H_{hh} represent the hole-particle, particle-particle, and hole-hole interactions, respectively. H' represents all remaining terms in the Hamiltonian and it will be ignored from now on since it will not give any contributions to matrix elements discussed in this paper. Two-body central forces are used for the calculation of the H_{hp} , H_{pp} , and H_{hh} matrix elements while the energy eigenvalues of H_{pC} and H_{hC} will be taken from experimental results as will be discussed in Sec. II F below.

B. Fermion states

The excited levels of the ^{16}O nucleus can be described as linear combinations of one-hole-one-particle states (1h-1p), two-hole-two-particle states (2h-2p), etc.

A (1h-1p) state will be written as

$$|\bar{h}_i p_k J T\rangle = [H_i^\dagger P_k^\dagger]^{J T} |0\rangle, \quad (2)$$

where the hole-creation operator H_i^\dagger and the particle-creation operator P_k^\dagger are coupled to a total angular momentum J and total isospin T and $|0\rangle$ is the closed core. The symbols h_i and p_i depict the

quantum numbers n , l , and j specifying a given hole orbital and a given particle orbital, respectively. All H 's and P 's satisfy the fermion anti-commutation relations so that all states satisfy the Pauli exclusion principle. The bar over h_i represents a hole in the core.

The states containing two holes and two particles can be formed in two ways. One way is first to couple two holes together and two particles together. Then one couples these two states together giving the (2h-2p) antisymmetric normalized wave function,

$$\begin{aligned} & |\bar{h}_1 \bar{h}_2 J_1 T_1\rangle (p_3 p_4 J_2 T_2) J T \rangle \\ &= \frac{[[H_1^\dagger H_2^\dagger]^{J_1 T_1} [P_3^\dagger P_4^\dagger]^{J_2 T_2}]^{J T} |0\rangle}{[1 + \delta(h_1 h_2)]^{1/2} [1 + \delta(p_3 p_4)]^{1/2}}. \quad (3) \end{aligned}$$

An alternative way is to couple two (1h-1p) states together giving

$$\begin{aligned} & |(\bar{h}_1 p_2 J_1 T_1)(\bar{h}_3 p_4 J_2 T_2) J T\rangle_N \\ &= N^{-1} [[H_1^\dagger P_2^\dagger]^{J_1 T_1} [H_3^\dagger P_4^\dagger]^{J_2 T_2}]^{J T} |0\rangle, \quad (4) \end{aligned}$$

where

$$\begin{aligned} N^2 &= 1 + \delta(J_1 J_2) \delta(T_1 T_2) \delta(h_1 h_3) \delta(p_2 p_4) \theta(J T) \\ &- (\hat{J}_1 \hat{J}_2 \hat{T}_1 \hat{T}_2)^2 \left\{ \begin{array}{c} \frac{1}{2} \quad \frac{1}{2} \quad T_1 \\ \frac{1}{2} \quad \frac{1}{2} \quad T_2 \\ T_1 \quad T_2 \quad T \end{array} \right\} \left(\delta(h_1 h_3) \left\{ \begin{array}{c} p_2 \quad h_1 \quad J_1 \\ h_1 \quad p_4 \quad J_2 \\ J_1 \quad J_2 \quad J \end{array} \right\} + \delta(p_2 p_4) \left\{ \begin{array}{c} h_1 \quad p_2 \quad J_1 \\ p_2 \quad h_3 \quad J_2 \\ J_1 \quad J_2 \quad J \end{array} \right\} \right) \end{aligned}$$

is the normalization factor expressed in terms of 9- j coefficients, Kronecker δ functions, and $\hat{x}^2 \equiv 2x + 1$. The wave function in Eq. (3) can be recoupled and written as a linear combination of the wave functions of Eq. (4) via a unitary transformation which involves four 9- J coefficients, two for isospin and two for angular momentum. Conversely, Eq. (4) can be expressed as a linear combination of the wave functions given by Eq. (3) and this will be done later in calculating the matrix elements of H_{pp} and H_{hh} .

C. Boson states

The one-boson states are obtained by diagonalizing the Hamiltonian in a (1h-1p) basis. In the work of FI and in this paper, the holes are restricted to the 1p shell and the particles are restricted to the 2s-1d shell. After diagonalizing, one has a spectrum of eigenstates with integer spin consisting of linear combinations of (1h-1p) states. These eigenstates are assumed to be bosons and will be written as

$$|b_i\rangle = B_i^\dagger |0\rangle = \sum_j w_{ij} |\bar{h}_j p_j J_i T_i\rangle, \quad (5)$$

where B_i^\dagger is a boson creation operator for the $J_i T_i$ state and obeys boson commutation rules.

Two-boson states can be formed by coupling two one-boson states together,

$$|b_1 b_2 J T\rangle = N_B^{-1} [B_1^\dagger B_2^\dagger]^{J T} |0\rangle, \quad (6)$$

where $N_B^2 = [1 + \delta(b_1 b_2)]$ and the boson creation operators B_1^\dagger and B_2^\dagger are coupled to J and T .

The two-boson states above can be written as a linear combination of products of (1h-1p) states using Eq. (5). Although the individual (1h-1p) states satisfy the Pauli exclusion principle, the product of two of them does not necessarily do so in general. One of the approximations in the IBA method is to assume that this violation of the Pauli principle is not important. The Pauli forbidden parts in these two-boson states, however, can be eliminated. The method used in this paper was to express the two-boson states as linear combinations of the (2h-2p) states given by Eq. (3). When

expressed as (2h-2p) states, the Pauli forbidden terms can be easily recognized, as these nonallowed components will have the configurations $(h^2J_1T_1)$ and/or $(p^2J_2T_2)$ with J_1+T_1 and/or J_2+T_2 even numbers. In the calculations described in Sec. V, these Pauli forbidden terms were eliminated from the two-boson states and the states were renormalized to have a unit norm before matrix elements of the Hamiltonian were calculated.

D. Matrix elements of H_{hp} , H_{pp} , and H_{hh}

Only H_{hp} has nonvanishing matrix elements between (1h-1p) states. The hole-particle matrix

$$G(j_1j_2j_3j_4JT) = \frac{\langle j_1j_2JT | V | j_3j_4JT \rangle + \theta(j_3j_4JT) \langle j_1j_2JT | V | j_4j_3JT \rangle}{[1 + \delta(j_1j_2)]^{1/2} [1 + \delta(j_3j_4)]^{1/2}}, \quad (8)$$

where $\theta(abc) = (-1)^{a+b+c}$. FI in Eqs. (3.4)–(3.8) and (3.21)–(3.25) of their Annals of Physics paper¹⁰ give expressions for the hole-particle and the two-particle matrix elements for a zero-range force. It appears that an overall phase of $\theta(j_1j_2j_3j_4)$ is missing from their $T=0$ and $T=1$ expressions for the two-particle matrix elements.

The two-boson states are given by a linear combination of (1h-1p) (1h-1p) states and so the matrix elements of H_{ph} , H_{pp} , and H_{hh} between two-boson states can be expressed as sums of matrix elements between (1h-1p) (1h-1p) states.

$$\begin{aligned} & \langle (\bar{h}_1 p_1 J_1 T_1) (\bar{h}_2 p_2 J_2 T_2) JT | H_{pp} + H_{hh} | (\bar{h}_3 p_3 J_3 T_3) (\bar{h}_4 p_4 J_4 T_4) JT \rangle \\ &= \hat{J}_1 \hat{J}_2 \hat{J}_3 \hat{J}_4 \hat{T}_1 \hat{T}_2 \hat{T}_3 \hat{T}_4 \sum_{J', J'', T', T''} (\hat{J}' \hat{J}'' \hat{T}' \hat{T}'')^2 \begin{Bmatrix} h_1 & p_1 & J_1 \\ h_2 & p_2 & J_2 \\ J' & J'' & J \end{Bmatrix} \begin{Bmatrix} h_3 & p_3 & J_3 \\ h_4 & p_4 & J_4 \\ J' & J'' & J \end{Bmatrix} \begin{Bmatrix} \frac{1}{2} & \frac{1}{2} & T_1 \\ \frac{1}{2} & \frac{1}{2} & T_2 \\ T' & T'' & T \end{Bmatrix} \begin{Bmatrix} \frac{1}{2} & \frac{1}{2} & T_3 \\ \frac{1}{2} & \frac{1}{2} & T_4 \\ T' & T'' & T \end{Bmatrix} \\ & \times \{ [\delta(h_1 h_3) \delta(h_2 h_4) + \theta(h_3 h_4 J' T') \delta(h_1 h_4) \delta(h_2 h_3)] [1 + \delta(p_1 p_2)]^{1/2} [1 + \delta(p_3 p_4)]^{1/2} \\ & \times G(p_1 p_2 p_3 p_4 J'' T'') + [\delta(p_1 p_3) \delta(p_2 p_4) + \theta(p_3 p_4 J'' T'') \delta(p_1 p_4) \delta(p_2 p_3)] \\ & \times [1 + \delta(h_1 h_2)]^{1/2} [1 + \delta(h_3 h_4)]^{1/2} G(h_1 h_2 h_3 h_4 J' T') \}. \quad (9) \end{aligned}$$

Equation (9) above is very similar to Eq. (3.15) given by Feshbach and Iachello¹⁰ but differs by factors of $[1 + \delta(p_1 p_2)]^{1/2} [1 + \delta(p_3 p_4)]^{1/2}$ and $[1 + \delta(h_1 h_2)]^{1/2} [1 + \delta(h_3 h_4)]^{1/2}$. These additional factors are necessary if $G(j_1 j_2 j_3 j_4 JT)$ is the standard matrix element between antisymmetric two-particle states. From inspection of Eq. (9), one can see that if there are any Pauli forbidden components in the two-boson wave functions, they will give a zero contribution to the H_{pp} and H_{hh} matrix elements as the brackets with the Kronecker δ functions will vanish.

The H_{hp} matrix elements are more complex and one needs to look at them in more detail in order to appreciate one of the major approximations of

element is given by

$$\begin{aligned} & \langle \bar{h}_1 p_1 JT | H_{hp} | \bar{h}_2 p_2 JT \rangle \\ &= - \sum_{J', T'} (\hat{J}' \hat{T}')^2 \begin{Bmatrix} h_1 p_1 J \\ h_2 p_2 J' \\ \frac{1}{2} \frac{1}{2} T \end{Bmatrix} \begin{Bmatrix} \frac{1}{2} \frac{1}{2} T' \end{Bmatrix} \\ & \times G(h_2 p_1 h_1 p_2 J' T') \quad (7) \end{aligned}$$

in terms of 6- J coefficients and the normalized two-particle matrix element between antisymmetric states, $G(j_1 j_2 j_3 j_4 JT)$. In terms of vector coupled states, $G(j_1 j_2 j_3 j_4 JT)$ is given by

$$\begin{aligned} & \langle (\bar{h}_1 p_2 J_1 T_1) (\bar{h}_3 p_4 J_2 T_2) JT \rangle \\ &= [[H_1^\dagger P_2^\dagger]^{J_1 T_1} [H_3^\dagger P_4^\dagger]^{J_2 T_2}]^{J T} | 0 \rangle \end{aligned}$$

and this state differs from the normalized (1h-1p) (1h-1p) state of Eq. (4) by the normalization factor N . The $H_{pp} + H_{hh}$ matrix element is

the IBA model. The matrix element

$$\langle (\bar{h}_1 p_1 J_1 T_1) (\bar{h}_2 p_2 J_2 T_2) JT | H_{hp} | (\bar{h}_3 p_3 J_3 T_3) (\bar{h}_4 p_4 J_4 T_4) JT \rangle$$

can be expanded in terms of 16 two-body matrix elements with suitable coefficients. It is readily seen that there will be four matrix elements of the form $\langle \bar{h}_i p_i J_i T_i | H_{hp} | \bar{h}_j p_j J_j T_j \rangle$ multiplied by Kronecker δ functions of the other quantum numbers. These four matrix elements will be labeled "direct matrix elements" and will be denoted by D_{hp} . The remaining 12 matrix elements will be labeled "exchange matrix elements" and will be denoted by X_{hp} . The X_{hp} matrix elements occur when a $|(\bar{h}_i p_i J_i T_i) (\bar{h}_j p_j J_j T_j) JT\rangle$ component in a two-bos-

on state is recoupled to a linear combination of $|\langle \bar{h}_i p_j J'T' \rangle \langle \bar{h}_j p_i J''T'' \rangle JT \rangle$ components giving rise to matrix elements which are of the form $\langle h_i p_j J'T' | H_{hp} | h_k p_l J''T'' \rangle$, where $i \neq j$ and/or $k \neq l$. The X_{hp} matrix elements will include either two or four $9-J$ coefficients along with other factors which arise from the recoupling. These X_{hp} matrix elements were neglected in the IBA model for reasons discussed below.

It should be noted that if the D_{hp} or X_{hp} matrix elements are calculated between two-boson states which have Pauli forbidden components in them, then the Pauli forbidden components will contribute to the D_{hp} or X_{hp} matrix elements. However, if the D_{hp} and X_{hp} matrix elements are calculated and added together, the contributions from the Pauli forbidden components cancel and will not contribute to the total H_{hp} matrix elements.

For computational reasons, the (1h-1p) (1h-1p) components of the two-boson states were recoupled to (2h-2p) components before the matrix elements of H_{hp} were calculated. The matrix element of H_{hp} between (2h-2p) states is given in the Appendix where the first 4 terms represent the D_{hp} contributions to the matrix element while the remaining 12 terms represent the X_{hp} contributions to the matrix element.

E. Spurious center of mass states

Whenever shell model calculations involve identical particles from two different major shells, there is always the possibility that spurious center-of-mass states will occur.¹¹⁻¹⁶ In these calculations, the five $(J, T) = (1^-, 0)$ one-boson states contain a spurious $1P$ center-of-mass state which was eliminated. The procedure^{15,16} used in this work was to add to the shell model Hamiltonian the term

$$H'_{c.m.} = A(H_{c.m.} - 3\hbar\omega/2) \quad (10)$$

and then diagonalize $H + H'_{c.m.}$ with the (1h-1p) basis. $H_{c.m.}$ is the center-of-mass Hamiltonian, A is the nuclear mass number (16 in this case), and $\hbar\omega$ is the harmonic oscillator spacing (13.92 MeV was used in these calculations). If a (1h-1p) state has no spurious center-of-mass components, $H'_{c.m.}$ will have a matrix element of zero. On the other hand, states with a large center-of-mass spuriousness will have matrix elements for $H'_{c.m.}$

of the order of $A\hbar\omega \approx 223$ MeV. With such a large energy separation, the states with a large center-of-mass spuriousness will not mix appreciably with those having a small center-of-mass spuriousness. In the calculation of the low lying $(J, T) = (1^-, 0)$ one-boson states in ^{16}O , this admixture was found to be much less than 1% verifying that this approach can effectively remove the center-of-mass spuriousness in the low lying states.

Even though the one-boson states have very little center-of-mass spuriousness in them, it is not guaranteed that the two-boson states will not have any. Since the two-bosons used do not span the complete $2\hbar\omega$ shell model space, one cannot eliminate the center-of-mass spuriousness by diagonalizing $H + H'_{c.m.}$. For the calculations described in this paper the amount of spurious center-of-mass motion in the two-boson states appears to be small as will be discussed later on.

F. Single particle energies and residual forces

The single particle energies in the $2s-1d$ shell and the single hole energies in the $1p$ shell were taken from experimental data in the ^{16}O region. In the ^{16}O , the Coulomb energies of a proton particle state and of a proton hole state almost cancel each other and so it is a good approximation to use the neutron energies for both neutrons and protons. The energies of the hole orbitals and particle orbitals are given in Table I.

The residual interaction used in the H_{hp} , H_{pp} , and H_{hh} matrix elements was assumed to be a central force of the form

$$V = \mathcal{U}(r)(W + MP^r + BP^s + HP^r P^s), \quad (11)$$

where P^r and P^s are the space and spin exchange operators, respectively. In order to see how sensitive the final results were to the residual force, calculations were done with the zero-range force used by FI and a short-ranged Gaussian force.

The zero-range force, V_{zr} , had a radial dependence of

$$\mathcal{U}(r) = V_0 \delta(\vec{r}_1 - \vec{r}_2)$$

and a Soper type admixture. The parameters of this force and the harmonic oscillator parameter $\nu = m\omega/\hbar$ used for the radial part of the single particle wave functions are given in Table II. The Gaussian force, V_G , had a radial dependence of

TABLE I. Single hole and single particle energies.

Orbital	$1\bar{p}_{3/2}$	$1\bar{p}_{1/2}$	$1d_{5/2}$	$2s_{1/2}$	$1d_{3/2}$
Energy (MeV)	21.85	15.67	-4.14	-3.27	0.94

TABLE II. Force parameters.

	Zero-range force	Gaussian force
V_0 (MeV)	-959	-40
W	0.365	0.65
M	0.365	0.65
B	0.135	0.15
H	0.135	0.15
ν (fm^{-2})	0.3228	0.3354
β (fm^{-2})	...	0.2922

$$V(r) = V_0 e^{-Br^2}$$

and the parameters for this force are given in Table II. Neither of these forces have singlet-odd or triplet-odd components. The V_{zr} force has a triplet-even to singlet-even ratio of 2.17 while the V_{G} force has a triplet-even to singlet-even ratio of 1.60.

The lowest $(J, T) = (3^-, 0)$ level in ^{16}O is expected to be due mainly to the $(1h-1p)$ configurations. Any admixtures of $(3h-3p)$ configurations are anticipated to be small and to have very little effect on the position of this level. The V_0 's of V_{zr} and V_{G} were chosen to give the lowest $(3^-, 0)$ level close to and slightly above the experimentally observed value of 6.13 MeV. A value of $V_0 = -959$ MeV for the zero-range force gave the lowest $(3^-, 0)$ level at 6.27 MeV while a $V_0 = -40$ MeV for the Gaussian force gave the lowest $(3^-, 0)$ level at 6.18 MeV. These levels and the other low lying $(1h-1p)$ levels will be discussed in more detail in Sec. III.

III. BOSON BASIS

The bosons used in the IBA model are the eigenstates resulting from diagonalizing the shell model Hamiltonian in a $(1h-1p)$ basis. As mentioned above, the holes were restricted to be in the $1p$ shell and the particles were restricted to be in the $2s-1d$ shell in this paper as well as in FI.

The spurious $1P$ center-of-mass state in the $(1^-, 0)$ spectrum was removed by the method described in Sec. II E. As was anticipated there, one $(1^-, 0)$ level moved up above 200 MeV and was found to have an overlap of 99.99% with the pure $1P$ spurious center-of-mass states. The other four $(1^-, 0)$ levels remained lower than 30 MeV and had negligible spuriousness in them.

The resulting $(1h-1p)$ spectrum for the zero-range and Gaussian forces are compared with the low lying experimentally observed levels¹⁷ in ^{16}O in Fig. 1. It is seen in this figure that for both the zero-range and Gaussian forces the lowest $(3^-, 0)$ and $(1^-, 0)$ levels are low lying and fairly well separated from the rather dense set of

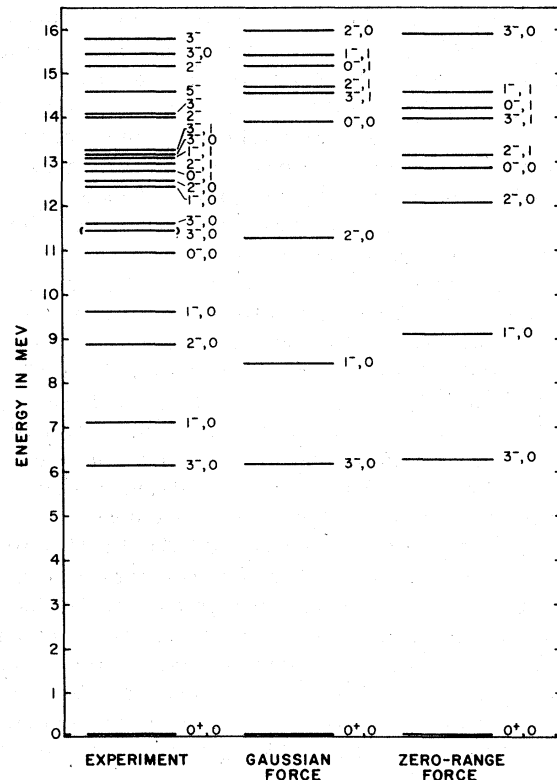


FIG. 1. Comparison of the calculated $(1h-1p)$ levels below 16 MeV for a Gaussian force and a zero-range force with the experimentally observed negative parity levels in ^{16}O (Ref. 17, Table 16.9).

negative parity lying above about 12 MeV. For the Gaussian force, the lowest $(2^-, 0)$ level at 11.2 MeV is also well separated by about 3 MeV from the more dense set of states above.

These two lowest $(1h-1p)$ eigenstates will assume to be the bosons to be used in the IBA model and one hopes to be able to describe the multiparticle excited states of ^{16}O by coupling these boson states together. The approach will be described in more detail in Secs. IV and V below.

It is interesting to explore the structure of the low lying $(3^-, 0)$ and $(1^-, 0)$ states in more detail. These two states are given in Table III for the zero-range and Gaussian forces and are compared with the FI results kindly sent to us by Iachello.¹⁸

In Table III, it is seen that the energies and the amplitudes of the $(1h-1p)$ components for the $(3^-, 0)$ level are essentially the same for the Gaussian force, the zero-range force calculated in this paper, and the zero-range force as calculated by Iachello.

The Gaussian force causes the lowest $(1^-, 0)$ level to lie about 1.5 MeV below the value that the zero-

TABLE III. Position and amplitudes of the lowest $(3^-, 0)$ and $(1^-, 0)$ states in ^{16}O for a zero-range force and a Gaussian force.

	$(3^-, 0)$ state zero-range force			$(1^-, 0)$ state zero-range force		
	Gaussian force	this calculation	Iachello	Gaussian force	this calculation	Iachello
Energy (MeV)	6.18	6.28	6.1	8.44	9.92	7.7
Configuration						
$(1\bar{p}_{1/2}1d_{5/2})$	0.85	0.87	0.87			
$(1\bar{p}_{3/2}1d_{3/2})$	-0.36	-0.33	-0.35	0.06	0.05	-0.17
$(1\bar{p}_{3/2}1d_{5/2})$	-0.39	-0.37	-0.35	0.30	0.28	-0.25
$(1\bar{p}_{1/2}2s_{1/2})$				0.77	0.85	0.62
$(1\bar{p}_{3/2}2s_{1/2})$				-0.51	-0.39	-0.61
$(1\bar{p}_{1/2}1d_{3/2})$				0.24	0.23	-0.37
Spuriousness				0.0008	0.0029	0.7613

range force gives even though the $(3^-, 0)$ levels were close together for the two forces. The amplitudes of the $(1^-, 0)$ states calculated for these two forces are essentially in agreement both in magnitude and sign. On the other hand, the lowest $(1^-, 0)$ level of Iachello¹⁸ differs substantially from the results obtained by the authors of this paper. Iachello's energy is 2.2 MeV lower and his amplitudes differ considerably in magnitude and sign. In fact, the overlap of Iachello's $(1^-, 0)$ eigenfunction with a pure spurious $1P$ center-of-mass state is 76% so that it does not appear that Iachello has correctly removed the spurious center-of-mass admixture in this eigenstate.

Since the authors of this paper do not have access to Iachello's calculation, it is difficult to speculate as to the probable cause of this discrepancy. Iachello¹⁰ diagonalized his shell model Hamiltonian in a space orthogonal to the $(1^-, 0)$ spurious state given by Elliott and Flowers¹ which should give states free of spurious center-of-mass motion. Firstly, Elliott and Flowers use a coupling scheme of $\vec{s} + \vec{l} = \vec{j}$ while this paper, FI, and Wang and Shakin¹⁹ (who also do a similar $(1h-1p)$ calculation in ^{16}O) use the coupling scheme of $\vec{l} + \vec{s} = \vec{j}$. Secondly, and perhaps more important, Elliott and Flowers use radial wave functions which decay positively to zero at large r . In their case, the radial wave functions start off positively (negatively) at the origin for odd (even) n quantum numbers. The usual convention is to use radial wave functions which start off positively at the origin and decay positively (negatively) at large r for odd (even) n . Since the results of this paper agree quite well for the lowest $(3^-, 0)$ state with the results of Iachello and Wang and Shakin, and for the lowest $(1^-, 0)$ state with the results of Wang and Shakin, it is assumed that all three are using the $\vec{l} + \vec{s} = \vec{j}$ convention and that the radial wave functions all start positively at the origin. If Iachello

used Elliot and Flower's spurious center-of-mass state without noting the above differences, then the spurious center-of-mass motion would not have been removed from the $(1^-, 0)$ wave functions. Otherwise, it is not possible at this time to resolve the differences between the two calculations with the same zero-range force.

IV. IBA MODEL

The interacting boson approximation model, was applied to the calculation of the lowest $0^+, 0$ and $2^+, 0$ levels in ^{16}O .

In order that the IBA be useful, one should be able to use only a few of the low lying one-boson states which when coupled together will form a "good" two-boson basis. In this paper and in FI, only the lowest $(3^-, 0)$ boson and the lowest $(1^-, 0)$ boson was used to form the two-boson basis. With these bosons, there are two two-boson states, $(3^-, 0)^2$ and $(1^-, 0)^2$, which can couple to a total J^π, T of $0^+, 0$, and there are three two-boson states, $(3^-, 0)^2$, $(1^-, 0)^2$, and $(3^-, 0)(1^-, 0)$, which can couple to a total J^π, T of $2^+, 0$. Consequently, one only has to diagonalize 2×2 and 3×3 matrices for the low lying $0^+, 0$ and $2^+, 0$ states of ^{16}O , respectively, as compared to 40×40 and 110×110 matrices, respectively, for exact $(2h-2p)$ calculations. But on the other hand, the two-boson matrix elements are more difficult to evaluate in general due to their more complex structure.

The IBA simplifies the calculation of the matrix elements in several ways. As has been pointed out above, when two bosons are coupled together, the resulting wave function can have Pauli forbidden components. In the IBA approach, it is assumed that the effects of the Pauli forbidden components will be small and can be neglected. As was mentioned in Sec. II D, the Pauli forbidden

components will give zero contribution to matrix elements of the $H_{pp} + H_{hh}$ parts of the Hamiltonian.

Even though the one-boson states have zero center-of-mass spuriousness in them, this will no longer be true when one couples two bosons together. The IBA neglects this possible center-of-mass admixture. Evidence will be presented below which indicates that there probably is only a small amount of center-of-mass admixture and that this approximation is valid.

The other important approximation of the IBA model concerns the matrix elements of H_{hp} . As was pointed out in Sec. IID above, the H_{hp} matrix elements can be split into two parts, the D_{hp} part which does not involve recoupling of the (1h-1p) (1h-1p) components of the wave functions and the X_{hp} part which does require recoupling of the (1h-1p) (1h-1p) components. The IBA model assumes that only the D_{hp} part of the matrix element is important and the X_{hp} part can be neglected. One reason for neglecting the X_{hp} part is that the recoupling introduces either two or four $9-J$ coefficients would make the X_{hp} part much smaller than the D_{hp} part. If this was the case, the X_{hp} part could be neglected without much error. The size of the D_{hp} and X_{hp} parts will be discussed in detail below. It can be pointed out, however, that it seems somewhat inconsistent to keep the $H_{pp} + H_{hh}$ parts of the matrix elements which involve four $9-J$ coefficients [see Eq. (9)] and neglect the X_{hp} parts which involve either two or four $9-J$ coefficients. FI argue that the neglect of the X_{hp} part is compensated by the neglect of the Pauli principle. Neglecting the X_{hp} parts will allow the Pauli forbidden components in the two-boson states to contribute to the matrix elements through

the D_{hp} part. Note that only when the D_{hp} and X_{hp} parts are added together will the Pauli forbidden contributions in each part cancel.

The matrix elements of $H_{pp} + H_{hh}$ and the D_{hp} part of the H_{hp} matrix elements have been calculated according to the IBA prescription and are given in Table IV where (30) and (10) symbolize $(3^-, 0)$ and $(1^-, 0)$, respectively. The X_{hp} parts, which would not normally be calculated in the IBA model, have been calculated and are given in Table IV in order that the size of D_{hp} , X_{hp} , $D_{hp} + X_{hp}$ and $H_{pp} + H_{hh}$ can be compared.

For both the Gaussian and zero-range forces, Table IV definitely shows that the X_{hp} parts of the matrix elements are not small compared to the D_{hp} parts. In fact, the X_{hp} parts are comparable in magnitude to the $H_{pp} + H_{hh}$ parts and are opposite in sign. Consequently, neglecting the X_{hp} terms does not appear to be a good approximation because the resulting states will lie too low in energy.

The $H_{pp} + H_{hh}$ matrix elements given by FI in Table II of their Annals of Physics paper¹⁰ do not agree with those of Table IV. One does not expect them to agree when the $(1^-, 0)$ boson state is involved as the $(1^-, 0)$ boson state of FI and the $(1^-, 0)$ boson state used in this paper differ substantially as discussed in Sec. III above. Since the $(3^-, 0)$ boson states are similar, one would expect to obtain similar matrix elements. The only reason which can be offered for the difference between the $(3^-, 0)^2$ JT diagonal matrix elements of FI and this paper is the phase factor difference in the two-particle matrix element in Eq. (8) and the square root factors appearing in Eq. (9) as discussed in Sec. IID.

TABLE IV. Matrix elements between two-boson states for the IBA model.

Matrix element	Boson energy	Gaussian force			Boson energy	Zero-range force		
		D_{hp}	X_{hp}	$H_{pp} + H_{hh}$		D_{hp}	X_{hp}	$H_{pp} + H_{hh}$
$0^+, 0$								
$(30)^2 - (30)^2$	12.35	-15.44	8.65	-7.04	12.56	-14.65	5.76	-7.58
$(30)^2 - (10)^2$		0.00	0.49	-1.43			0.64	-1.79
$(10)^2 - (10)^2$	16.88	-12.43	9.06	-9.49	19.84	-8.14	5.37	-8.02
$2^+, 0$								
$(30)^2 - (30)^2$	12.35	-15.44	6.47	-5.13	12.56	-14.65	4.06	-4.70
$(30)^2 - (30)(10)$		0.00	-0.95	0.08		0.00	-0.95	0.20
$(30)^2 - (10)^2$		0.00	0.14	-0.52		0.00	0.24	-0.67
$(30)(10) - (30)(10)$	14.62	-13.94	7.17	-5.73	16.20	-11.40	4.75	-4.38
$(30)(10) - (10)^2$		0.00	-1.93	1.87		0.00	-1.50	1.27
$(10)^2 - (10)^2$	16.88	-12.43	8.97	-7.04	19.84	-8.14	6.28	-5.64

V. EBA MODEL

In the previous section, it was seen that the X_{hp} parts of the matrix elements were not negligible compared to the D_{hp} parts of the $H_{pp} + H_{hh}$ matrix elements which raises questions about the validity of the IBA approximations. From the D_{hp} and X_{hp} parts of the matrix elements given in Table IV, it is not possible to determine how much of a contribution was due to the Pauli forbidden components in the two-boson basis states.

Consequently, a more complete calculation was undertaken in order to clear up some of the above questions and to see if a more complete and accurate description of the low lying positive parity states of ^{16}O could be obtained while retaining the desirable features of the IBA model. This more complete calculation will be called the extended boson approximation, EBA.²⁰

In the EBA model as in the IBA model, it will be assumed that only a few two-boson states are needed and that these few two-boson states will contain the important (2h-2p) configurations in the excited states. In contrast to the IBA model, the EBA model will satisfy the Pauli principle by eliminating the Pauli nonallowed components. In this paper, these nonallowed components were eliminated after recoupling the two-boson states so that their components could be written in the (2h-2p) scheme as described in Sec. II C above.

In the microscopic picture, the two-boson states do not have a norm of unity even with the boson normalization of Eq. (6). This deviation from a unit norm comes from the third term of the microscopic normalization factor N in Eq. (4) and this third term is absent in the boson normalization.

In the present calculations, the overlap between the boson-normalized two-boson states ranged from 1.008 to 0.835. After deletion of the Pauli forbidden terms, the resulting two-boson states were renormalized to a unit norm. These modified two-boson states in the EBA model will be called extended two-boson states to distinguish them from the two-boson states of the IBA model. Because the Pauli forbidden components have been removed, the various extended two-boson basis states will no longer, in general, be orthogonal to each other.

The boson energies in the IBA model gave the matrix elements of H_{pC} and H_{hC} and the direct part of the H_{hp} . In the EBA model, the matrix elements of $H_{pC} + H_{hC}$ between the extended two-boson states were evaluated directly. The final difference between the two approaches is that in the EBA model both the D_{hp} and the X_{hp} parts of the matrix elements of H_{hp} between the extended two-boson states are kept.

As with the calculations using the IBA model described in the previous section, the $(3^-, 0)$ and $(1^-, 0)$ bosons were used to construct the $0^+, 0$ and $2^+, 0$ two-boson basis states. Then the Pauli nonallowed terms were eliminated and the states renormalized to produce the extended two-boson basis states. Using these extended two-boson states, the matrix elements of $H_{pC} + H_{hC}$, $H_{pp} + H_{hh}$, and the D_{hp} and X_{hp} parts of H_{hp} were calculated for the Gaussian force and the zero-range force. These matrix elements are given in Table V and several interesting remarks can be made. Compared to the D_{hp} parts of the diagonal matrix elements in the IBA model, the D_{hp} parts in the EBA model are drastically reduced

TABLE V. Matrix elements between the extended two-boson states for the EBA model. E_0 is the matrix element of $H_{pC} + H_{hC}$ between the extended two-boson states.

Matrix element	Gaussian force				Zero-range force			
	E_0	D_{hp}	X_{hp}	$H_{pp} + H_{hh}$	E_0	D_{hp}	X_{hp}	$H_{pp} + H_{hh}$
				0 ⁺ , 0				
(30) ² -(30) ²	27.54	-4.18	-2.54	-6.97	26.95	-4.42	-4.33	-7.45
(30) ² -(10) ²	-0.97	0.05	0.47	-1.52	-0.76	0.05	0.60	-1.81
(10) ² -(10) ²	28.44	-2.77	-1.12	-10.95	26.95	-1.97	-0.90	-8.33
				2 ⁺ , 0				
(30) ² -(30) ²	27.81	-4.70	-4.20	-5.09	27.22	-4.82	-5.69	-4.66
(30) ² -(30)(10)	0.85	-0.22	-0.74	0.08	0.75	-0.21	-0.73	0.20
(30) ² -(10) ²	-0.44	0.02	0.14	0.60	-0.39	0.02	0.27	-0.79
(30)(10)-(30)(10)	28.37	-6.52	-0.38	-5.84	27.28	-5.09	-1.58	-4.39
(30)(10)-(10) ²	3.79	-0.08	-2.16	2.17	2.80	-0.03	-1.78	1.52
(10) ² -(10) ²	30.30	-3.52	-1.06	-9.32	28.91	-2.64	-0.03	-8.09

in size due to the elimination of the Pauli nonallowed components in the two-boson states. The X_{np} parts of the diagonal matrix elements in the EBA model are not only reduced in size but are opposite in sign from the IBA results. The sum of the D_{np} and X_{np} parts are essentially the same for both models with the small differences arising from normalization. Consequently, it is seen that the Pauli nonallowed terms make a big difference in the D_{np} and X_{np} matrix elements. Since the Pauli nonallowed terms do not contribute to the $H_{pp} + H_{hh}$ matrix elements, the small differences between them in the two models are due to the differences between the boson and exact normalizations.

In the IBA model, the only contribution to the off-diagonal matrix elements come from the $H_{pp} + H_{hh}$ part of the Hamiltonian. In both models, the calculated X_{np} parts tend to cancel the $H_{pp} + H_{hh}$ part making the off-diagonal matrix elements smaller than if the X_{np} part were neglected. Because of the smaller off-diagonal matrix elements in the EBA calculations, there will be less mixing of the two-boson states after diagonalization in the EBA model than in the IBA model. However, this effect will be negligible due to the large energy separation of the diagonal matrix elements in both models.

In both the IBA model and the EBA model, the two-boson states can have some center-of-mass spuriousness in them even though the original one-boson states were free of center-of-mass motion. Although the spuriousness of these states cannot be readily removed, a fairly good estimate of the spuriousness can be obtained by evaluating the expectation value of $AH_{c.m.}$ between the extended two-boson states. It was found that $\langle AH_{c.m.} \rangle$ ranged from 2 to 8 MeV making $\langle AH_{c.m.} \rangle / A\hbar\omega \approx 0.009$ to 0.036 which indicates very little spurious center-of-mass motion in these states.

With all the relevant matrix elements, one can now diagonalize the shell model Hamiltonian with the two-boson basis states in the IBA model and the EBA model. In the EBA case, the nonorthogonality of the extended two-boson basis states was taken into account in the diagonalization process. The results of the diagonalization for the two models will be compared with an exact (2h-2p) calculation of the lowest $0^+, 0$ and $2^+, 0$ levels in ^{16}O in the next section.

VI. EXACT (2h-2p) CALCULATIONS

For the IBA model and the EBA model to be able to describe the low lying excited positive parity levels in ^{16}O , the energies and microscopic structure resulting after diagonalization should be

similar to the results obtained when an exact calculation is done. That is, not only should similar energy eigenvalues be obtained but the larger dominant components of the eigenstates should be the same.

With holes in the $1p$ shell and particles in the $2s-1d$ shell, and the same Gaussian and zero-range forces used previously, $H + H'_{c.m.}$ was diagonalized in a complete 2h-2p basis for the $0^+, 0$ and $2^+, 0$ states. By diagonalizing $H + H'_{c.m.}$, it is believed that the spurious center-of-mass admixtures were removed from the low lying states. However, the amount of spuriousness in the low lying states was not checked by calculating their overlaps with the spurious $1S-2D$ state or the spurious $1P$ states. In the $0^+, 0$ spectrum for example, one eigenstate appeared around 400 MeV while four eigenstates appeared around 200 MeV and these five eigenstates presumably contain most of the spurious center-of-mass motion. One can account for the appearance of these five states by using the fact that in the 1h-1p space, there is one $1P$ spurious state and four nonspurious states. The $1P$ state could couple with itself a form a $2S-1D$ spurious state of energy $2\hbar\omega$ which one identifies with the $0^+, 0$ eigenstate near 400 MeV in the (2h-2p) spectrum. The $1P$ spurious state can couple with the other four nonspurious states to produce four $1P$ spurious states of energy $1\hbar\omega$ which one identifies with the four $0^+, 0$ eigenstates around 200 MeV. That these 5 eigenstates are well separated in energy from the remaining 35 lower lying eigenstates is evidence that these lower lying eigenstates contain very little spurious center-of-mass motion. Similar remarks can be made about the $2^+, 0$ eigenstates where one spurious eigenstate appears around 400 MeV and 12 spurious eigenstates appear around 200 MeV.

The results for the exact calculation, the IBA calculation, and the EBA calculation are compared in Tables VI-VIII. The lower lying $0^+, 0$ and $2^+, 0$ energy levels are compared with the experimental positive parity levels in ^{16}O in Fig. 2.

The exact calculation gives the lowest $0^+, 0$ level at 9.08 MeV for the Gaussian force and at 4.88 MeV for the zero-range force as compared to the observed $0^+, 0$ level at 6.05 MeV. If this observed state was entirely due to 2h-2p configurations, then the Gaussian force would be too weak and the zero-range force would be too strong. One believes that there is substantial (4h-4p) admixture in this state and inclusion of these (4h-4p) configurations would tend to push the calculated levels lower making the Gaussian force results closer to the experimental results and the zero-range results further away. On the other hand, the 1 MeV difference between the exact zero-

TABLE VI. Energies and dominant configurations of the lowest $0^+, 0$ eigenstates for the exact calculation, the IBA model, and the EBA model. Configurations whose amplitude is less than 1% in any of the calculations are not included. The lower observed $0^+, 0$ level in ^{16}O is at 6.05 MeV. The components marked by an asterisk do not occur in the two-boson states.

Configurations	Energy in MeV	Gaussian force			Zero-range force		
		Exact 9.08	IBA 4.59	EBA 12.18	Exact 4.88	IBA 4.54	EBA 10.26
$(p_{1/2}^2 01)$	$(d_{5/2}^2 01)$	-0.55	-0.60	-0.46	-0.44	-0.69	-0.68
$(p_{1/2}^2 10)$	$(d_{5/2}^2 10)$	0.15	0.29	0.23	0.20	0.33	0.33
$(p_{1/2}^2 10)$	$(d_{5/2} d_{3/2} 10)$	-0.17	*	*	-0.23	*	*
$(p_{1/2}^2 01)$	$(d_{3/2}^2 01)$	-0.14	-0.19	-0.03	-0.08	-0.01	-0.01
$(p_{1/2}^2 01)$	$(s_{1/2}^2 01)$	-0.24	-0.28	-0.50	-0.09	-0.18	-0.22
$(p_{1/2}^2 10)$	$(s_{1/2}^2 10)$	0.11	0.09	0.17	0.11	0.06	0.07
$(p_{1/2} p_{3/2} 10)$	$(d_{5/2}^2 10)$	-0.35	-0.24	-0.19	-0.44	-0.25	-0.25
$(p_{1/2} p_{3/2} 21)$	$(d_{5/2}^2 21)$	0.02	0.30	0.23	0.14	0.31	0.31
$(p_{1/2} p_{3/2} 10)$	$(d_{5/2} d_{3/2} 10)$	0.32	0.20	0.17	0.42	0.20	0.19
$(p_{1/2} p_{3/2} 11)$	$(d_{5/2} d_{3/2} 11)$	0.13	0.28	0.18	0.17	0.31	0.30
$(p_{1/2} p_{3/2} 21)$	$(d_{5/2} s_{1/2} 21)$	-0.14	0.00	0.00	-0.07	0.00	0.00
$(p_{1/2} p_{3/2} 10)$	$(d_{3/2}^2 10)$	0.08	0.00	0.00	0.11	0.00	0.00
$(p_{1/2} p_{3/2} 10)$	$(s_{1/2}^2 10)$	-0.24	-0.18	-0.31	-0.20	-0.08	-0.10
$(p_{3/2}^2 01)$	$(d_{5/2}^2 01)$	-0.24	-0.11	-0.10	-0.16	-0.10	-0.10
$(p_{3/2}^2 10)$	$(d_{5/2}^2 10)$	-0.14	-0.02	-0.03	-0.18	0.00	0.00
$(p_{3/2}^2 10)$	$(d_{5/2} d_{3/2} 10)$	0.19	0.09	0.07	0.26	0.09	0.09
$(p_{3/2}^2 21)$	$(d_{5/2} d_{3/2} 21)$	-0.04	-0.13	-0.09	-0.08	-0.13	-0.12
$(p_{3/2}^2 01)$	$(d_{3/2}^2 01)$	-0.13	-0.09	-0.07	-0.11	-0.09	-0.09
$(p_{3/2}^2 30)$	$(d_{5/2}^2 30)$	0.10	0.07	0.12	-0.07	0.02	0.03
$(p_{3/2}^2 01)$	$(s_{1/2}^2 01)$	-0.13	-0.09	-0.16	-0.04	-0.03	-0.03
$(p_{3/2}^2 10)$	$(s_{1/2}^2 10)$	-0.13	-0.07	-0.12	-0.11	-0.02	-0.03

range results and the observed position of 6.05 MeV is not a serious disagreement for this region of the periodic table.

For all six calculations of the lowest $0^+, 0$ level, the amplitudes follow similar trends in sign and magnitude. However, for both the Gaussian force and the zero-range force the IBA and EBA amplitudes are sufficiently different from the exact results so that there is only a 50% to 60% overlap between the wave functions of the exact results and those of the IBA and EBA results. One normally requires a 95% or better overlap before it can be said that the wave functions agree. So the small overlaps above indicate non-agreement.

In the exact calculation, the lowest $2^+, 0$ eigenstate is at 11.25 MeV for the Gaussian force and at 9.74 MeV for the zero-range force both of which are above the observed position of 6.92 MeV. The IBA model gives the energy level fairly

close to the observed value for both forces while the EBA results are too high.

The amplitudes of the lowest $2^+, 0$ state for both forces in the IBA and EBA cases are in poorer agreement with the exact results than was the case for the $0^+, 0$ results. Not only is there disagreement in signs for some amplitudes, but some amplitudes in the exact case are large (small) while those in the IBA and EBA cases are small (large). It should be noted that the amplitudes of the exact calculations do not even agree for the two forces indicating a sensitivity to the force used. The exact zero-range force results have two relatively large amplitudes which do not appear in the two-boson basis states and which are less than 1% in the exact Gaussian force results.

Thus, it appears that there is rather poor agreement between the exact calculations and both the IBA and EBA results. With sensitivity to the force

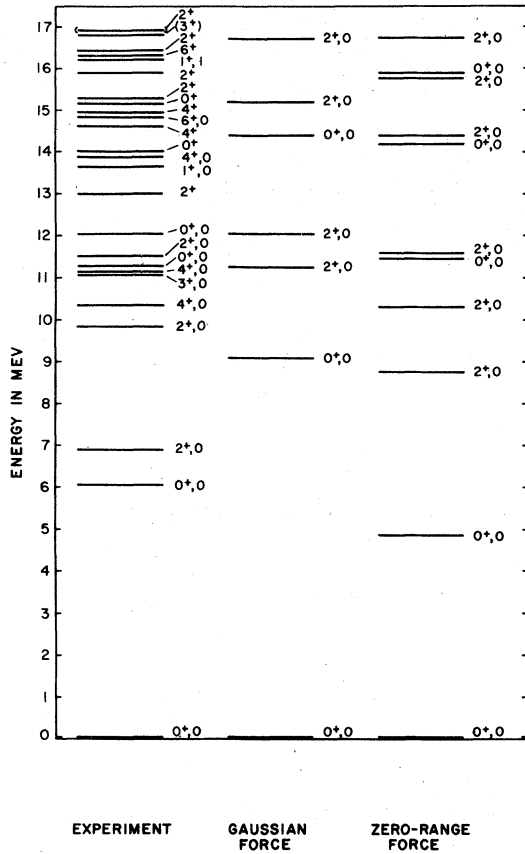


FIG. 2. Comparison of the low lying 0^+0 and 2^+0 levels from exact (2h-2p) calculations for a Gaussian force and a zero-range force with the experimentally observed positive parity states below 17 MeV (Ref. 17, Table 16.9).

and the generally poor agreement between the results of the calculations, one is not encouraged to proceed further and consider (4h-4p) admixtures arising from four boson states or to calculate transition rates between states.

VII. CONCLUSIONS

In this paper, the interacting boson approximation and a modification of it, the extended boson approximation, was compared with exact (2h-2p) calculations of the position and structure of the lowest $0^+,0$ and $2^+,0$ states of ^{16}O . The EBA model was used to examine the effects of two questionable approximations made by the IBA model which are the neglect of the Pauli principle and the neglect the recoupled parts of the H_{hp} matrix elements.

The results indicated that both of these approximations of the IBA model are not valid and result in large changes in the matrix elements from what is the case for the more exact EBA calculation. Furthermore, neither the IBA model nor the EBA model agree sufficiently well with complete exact (2h-2p) shell model calculations so one concludes that neither of them is a good model to describe the low lying positive parity states of ^{16}O .

These results do not, however, preclude the possibility that the IBA or EBA approaches might work better for nuclei in other regions of the periodic table. Recently Iachello and Arima^{21,22} have developed an interacting boson approach in which collective nuclear states are described by a Hamiltonian written in terms of $l=0$ and $l=2$ bosons and interactions between them. This approach appears to be able to describe vibrational and rotational states of deformed nuclei.

APPENDIX

The matrix element of H_{hp} between two (2h-2p) states can be written as a sum of 16 terms. Only the first term denoted as \mathfrak{M} will be explicitly given. The remaining 15 terms can easily be calculated with the expression for \mathfrak{M} by suitable interchange of quantum numbers as described below.

Let lower case Roman letters refer to the particles with the letter b denoting $(n_b l_b j_b)$ and lower case Greek letter referring to holes with the letter α denoting $(n_\alpha l_\alpha j_\alpha)$. If b or α appears in $\theta(abc) \equiv (-1)^{a+b+c}$, in a 6- J or 9- J coefficient, etc., it is understood to denote j_b or j_α , respectively. $\mathfrak{M}(\alpha \rightleftharpoons \beta)$ means that the quantum numbers α and β appearing in \mathfrak{M} are to be interchanged before \mathfrak{M} is evaluated. Similarly, $\mathfrak{M}(\alpha \rightleftharpoons \beta, a \rightleftharpoons b)$ means that the α and β quantum numbers and the a and b quantum numbers are to be interchanged.

The matrix element for H_{hp} can be written as

TABLE VII. Energies and dominant configurations of the lowest $2^+, 0$ eigenstate obtained with the Gaussian force. The lowest observed $2^+, 0$ level in ^{16}O is at 6.92 MeV.

Configurations		Energy in MeV	Exact 11.25	IBA 6.91	EBA 13.47
$(p_{1/2}^2 01)$	$(d_{5/2}^2 21)$		-0.40	-0.50	-0.39
$(p_{1/2}^2 10)$	$(d_{5/2}^2 10)$		-0.07	-0.26	-0.20
$(p_{1/2}^2 10)$	$(d_{5/2}^2 30)$		0.13	0.13	0.10
$(p_{1/2}^2 10)$	$(d_{5/2} d_{3/2} 10)$		-0.11	0.04	0.06
$(p_{1/2}^2 01)$	$(d_{5/2} s_{1/2} 21)$		-0.40	0.26	0.36
$(p_{1/2}^2 10)$	$(d_{5/2} s_{1/2} 30)$		0.19	-0.03	-0.05
$(p_{1/2}^2 01)$	$(d_{3/2} s_{1/2} 21)$		0.15	-0.08	-0.14
$(p_{1/2} p_{3/2} 10)$	$(d_{5/2}^2 10)$		0.10	0.08	0.06
$(p_{1/2} p_{3/2} 10)$	$(d_{5/2}^2 30)$		-0.21	-0.17	-0.14
$(p_{1/2} p_{3/2} 21)$	$(d_{5/2}^2 21)$		-0.16	-0.11	-0.04
$(p_{1/2} p_{3/2} 10)$	$(d_{5/2} d_{3/2} 20)$		-0.17	-0.12	-0.10
$(p_{1/2} p_{3/2} 10)$	$(d_{5/2} s_{1/2} 20)$		-0.18	0.07	0.09
$(p_{1/2} p_{3/2} 10)$	$(d_{5/2} s_{1/2} 30)$		-0.31	0.14	0.21
$(p_{1/2} p_{3/2} 10)$	$(d_{3/2} s_{1/2} 10)$		-0.12	0.04	0.11
$(p_{1/2} p_{3/2} 20)$	$(d_{3/2} s_{1/2} 20)$		-0.12	0.04	0.06
$(p_{3/2}^2 01)$	$(d_{5/2}^2 21)$		-0.15	-0.06	-0.06
$(p_{3/2}^2 10)$	$(d_{5/2}^2 30)$		-0.11	-0.04	-0.04
$(p_{3/2}^2 01)$	$(d_{5/2} s_{1/2} 21)$		-0.19	0.07	0.11
$(p_{3/2}^2 10)$	$(d_{5/2} s_{1/2} 30)$		-0.18	0.05	0.07
$(p_{3/2}^2 01)$	$(d_{3/2} s_{1/2} 21)$		0.12	-0.05	-0.07

$$\begin{aligned}
& \langle (\bar{\alpha}\bar{\beta}J_1 T_1)(abJ_2 T_2)JT | H_{hp} | (\bar{\gamma}\bar{\delta}J_3 T_3)(cdJ_4 T_4)JT \rangle \\
& = \mathfrak{M} + \theta(\alpha\beta abJ_1 T_1 J_2 T_2) \mathfrak{M}(\alpha \bar{\alpha} \beta, a \bar{a} b) + \theta(\gamma\delta cdJ_3 T_3 J_4 T_4) \mathfrak{M}(\gamma \bar{\gamma} \delta, c \bar{c} d) \\
& + \theta(\alpha\beta\gamma\delta abcdJ_1 T_1 J_2 T_2 J_3 T_3 J_4 T_4) \mathfrak{M}(\alpha \bar{\alpha} \beta, \gamma \bar{\gamma} \delta, a \bar{a} b, c \bar{c} d) \\
& + \theta(\alpha\beta J_1 T_1) \mathfrak{M}(\alpha \bar{\alpha} \beta) + \theta(\gamma\delta J_3 T_3) \mathfrak{M}(\gamma \bar{\gamma} \delta) + \theta(abJ_2 T_2) \mathfrak{M}(a \bar{a} b) + \theta(cdJ_4 T_4) \mathfrak{M}(c \bar{c} d) \\
& + \theta(\alpha\beta cdJ_1 T_1 J_4 T_4) \mathfrak{M}(\alpha \bar{\alpha} \beta, c \bar{c} d) + \theta(\gamma\delta abJ_2 T_2 J_3 T_3) \mathfrak{M}(\gamma \bar{\gamma} \delta, a \bar{a} b) \\
& + \theta(abcdJ_2 T_2 J_4 T_4) \mathfrak{M}(a \bar{a} b, c \bar{c} d) + \theta(\alpha\beta\gamma\delta J_1 T_1 J_3 T_3) \mathfrak{M}(\alpha \bar{\alpha} \beta, \gamma \bar{\gamma} \delta) \\
& + \theta(\alpha\beta\gamma\delta abJ_1 T_1 J_2 T_2 J_3 T_3) \mathfrak{M}(\alpha \bar{\alpha} \beta, \gamma \bar{\gamma} \delta, a \bar{a} b) + \theta(\alpha\beta\gamma\delta cdJ_1 T_1 J_3 T_3 J_4 T_4) \mathfrak{M}(\alpha \bar{\alpha} \beta, \gamma \bar{\gamma} \delta, c \bar{c} d) \\
& + \theta(\alpha\beta abcdJ_1 T_1 J_2 T_2 J_4 T_4) \mathfrak{M}(\alpha \bar{\alpha} \beta, a \bar{a} b, c \bar{c} d) + \theta(\gamma\delta abcdJ_2 T_2 J_3 T_3 J_4 T_4) \mathfrak{M}(\gamma \bar{\gamma} \delta, a \bar{a} b, c \bar{c} d). \quad (A1)
\end{aligned}$$

The reduction of the (2h-2p) matrix element to the form given by Eq. (A1) proceeds in the same way as a similar derivation done by True and Ma⁸ where isospin was not included.

For conciseness in giving the relation for \mathfrak{M} , the following notation will be used:

$$\rho \equiv - \frac{\delta(\beta\delta)\delta(bd)\hat{a}\hat{c}\hat{\alpha}\hat{\gamma}\hat{J}_1\hat{J}_2\hat{J}_3\hat{J}_4\hat{T}_1\hat{T}_2\hat{T}_3\hat{T}_4\theta(\alpha\beta\gamma abcJ_2 J_4 J T_1 T_3 l_a l_\gamma)}{[1 + \delta(\alpha\beta)][1 + \delta(\gamma\delta)][1 + \delta(ab)][1 + \delta(cd)]^{1/2}}, \quad (A2)$$

$$\sigma \equiv \theta(T'), \quad (A3)$$

$$\lambda(x) \equiv \begin{Bmatrix} c & a & x \\ J_2 & J_4 & b \end{Bmatrix} \begin{Bmatrix} J_2 & J_4 & x \\ J_3 & J_1 & J \end{Bmatrix} \begin{Bmatrix} \alpha & \gamma & x \\ J_3 & J_1 & \beta \end{Bmatrix}, \quad (A4)$$

TABLE VIII. Energies and dominant configurations of the lowest $2^+, 0$ eigenstate obtained with the zero-range force. The components marked by an asterisk do not occur in the two-boson states.

Configurations		Energy in MeV	Exact	IBA	EBA
			8.74	7.77	11.95
$(p_{1/2}^2 01)$	$(d_{5/2}^2 21)$		-0.46	-0.65	-0.65
$(p_{1/2}^2 10)$	$(d_{5/2}^2 10)$		-0.20	-0.33	-0.33
$(p_{1/2}^2 10)$	$(d_{5/2}^2 30)$		-0.06	0.17	0.17
$(p_{1/2}^2 10)$	$(d_{5/2} d_{3/2} 10)$		0.39	0.01	-0.002
$(p_{1/2}^2 10)$	$(d_{5/2}^2 10)$		0.12	*	*
$(p_{1/2}^2 10)$	$(s_{1/2}^2 10)$		-0.28	-0.06	-0.07
$(p_{1/2} p_{3/2} 10)$	$(d_{5/2}^2 10)$		0.34	0.11	0.11
$(p_{1/2} p_{3/2} 21)$	$(d_{5/2}^2 01)$		0.13	0.24	0.23
$(p_{1/2} p_{3/2} 20)$	$(d_{5/2}^2 30)$		-0.17	-0.03	-0.04
$(p_{1/2} p_{3/2} 21)$	$(d_{5/2}^2 21)$		-0.11	-0.20	-0.22
$(p_{1/2} p_{3/2} 10)$	$(d_{5/2} d_{3/2} 10)$		-0.28	0.09	0.09
$(p_{1/2} p_{3/2} 10)$	$(s_{1/2}^2 10)$		0.22	-0.01	-0.01
$(p_{3/2}^2 10)$	$(d_{5/2}^2 10)$		0.21	-0.04	-0.04
$(p_{3/2}^2 10)$	$(d_{5/2} d_{3/2} 10)$		-0.22	*	*
$(p_{3/2}^2 10)$	$(s_{1/2}^2 10)$		0.16	0.002	0.002

$$\phi_D(k) \equiv R^k(l_a l_\gamma l_\alpha l_c) \langle l_a || C^k || l_\alpha \rangle \langle l_\gamma || C^k || l_c \rangle, \quad (\text{A5})$$

and

$$\phi_X(k) \equiv R^k(l_a l_\gamma l_\alpha l_c) \langle l_a || C^k || l_c \rangle \langle l_\gamma || C^k || l_\alpha \rangle, \quad (\text{A6})$$

where $R^k(l_1 l_2 l_3 l_4)$ is the conventional Slater integral and $\langle l_1 || C^k || l_2 \rangle$ is the reduced matrix element of $C_q^k \equiv [4\pi/(2k+1)]^{1/2} Y_q^k(\theta, \phi)$.

In terms of a $12\text{-}J$ coefficient and the definitions in (A2)-(A6), \mathfrak{M} is given by

$$\begin{aligned} \mathfrak{M} = \rho \sum_{T'} \sigma \hat{T}'^2 \left\{ \begin{array}{cc} \frac{1}{2} & \frac{1}{2} & T_4 & T_3 \\ \frac{1}{2} & T' & \frac{1}{2} & T_1 \\ T_2 & \frac{1}{2} & T & \frac{1}{2} \end{array} \right\} & \left((W + \sigma H) \sum_{k,x} \theta(k) \hat{x}^2 \lambda(x) \phi_D(k) \begin{Bmatrix} \gamma & \alpha & x \\ a & c & k \end{Bmatrix} \begin{Bmatrix} a & \alpha & k \\ l_\alpha & l_a & \frac{1}{2} \end{Bmatrix} \begin{Bmatrix} \gamma & c & k \\ l_c & l_\gamma & \frac{1}{2} \end{Bmatrix} \right. \\ & - (B + \sigma M) \sum_{k,x} \theta(k) \hat{x}^2 \lambda(x) \phi_D(k) \begin{Bmatrix} l_c & l_\gamma & k \\ l_\alpha & l_a & x \end{Bmatrix} \begin{Bmatrix} l_\gamma & l_\alpha & x \\ \alpha & \gamma & \frac{1}{2} \end{Bmatrix} \begin{Bmatrix} l_a & l_c & x \\ c & a & \frac{1}{2} \end{Bmatrix} \\ & - (H + \sigma W) \sum_k \theta(k) \lambda(k) \phi_X(k) \begin{Bmatrix} a & c & k \\ l_c & l_a & \frac{1}{2} \end{Bmatrix} \begin{Bmatrix} \gamma & \alpha & k \\ l_\alpha & l_\gamma & \frac{1}{2} \end{Bmatrix} \\ & + (M + \sigma B) \sum_{k,x,q} \theta(k) \hat{x}^2 \hat{q}^2 \lambda(x) \phi_X(k) \\ & \left. \times \begin{Bmatrix} \alpha & \gamma & x \\ c & a & q \end{Bmatrix} \begin{Bmatrix} l_a & l_\alpha & q \\ \alpha & a & \frac{1}{2} \end{Bmatrix} \begin{Bmatrix} l_\gamma & l_c & q \\ c & \gamma & \frac{1}{2} \end{Bmatrix} \begin{Bmatrix} l_a & l_c & k \\ l_\gamma & l_\alpha & q \end{Bmatrix} \right). \quad (\text{A7}) \end{aligned}$$

- [†]Based on a Ph.D. thesis submitted to the University of California, Davis, California in September, 1976 by F. Darema-Rogers (unpublished).
- *Present address: Physics Department, Brookhaven National Laboratory, Upton, New York 11973.
- ¹J. P. Elliott and B. H. Flowers, Proc. R. Soc. London A229, 536 (1955); A242, 57 (1957).
- ²W. W. True and K. W. Ford, Phys. Rev. 109, 1675 (1958).
- ³T. T. S. Kuo and G. E. Brown, Nucl. Phys. 85, 40 (1966); G. H. Herling and T. T. S. Kuo, *ibid.* A181, 113, (1972).
- ⁴E. C. Halbert, J. B. McGrory, and B. H. Wildenthal, Phys. Rev. Lett. 20, 1112 (1968).
- ⁵A. P. Zuker, B. Buck, and J. B. McGrory, Phys. Rev. Lett. 21, 39 (1968).
- ⁶J. B. McGrory and T. T. S. Kuo, Nucl. Phys. A247, 283 (1975).
- ⁷N. K. Glendenning and K. Harada, Nucl. Phys. 72, 481 (1965).
- ⁸W. W. True and C. W. Ma, Phys. Rev. C 9, 2275 (1974).
- ⁹F. Iachello, Ph.D. thesis, MIT, 1969 (unpublished).
- ¹⁰H. Feshbach and F. Iachello, Phys. Lett. 45B, 7 (1973); Ann. Phys. (NY) 84, 211 (1974).
- ¹¹S. Gartenhaus and C. Schwartz, Phys. Rev. 108, 482 (1957).
- ¹²J. P. Elliott and T. H. R. Skyrme, Proc. R. Soc. London A232, 561 (1955).
- ¹³E. Baranger and C. W. Lee, Nucl. Phys. 22, 157 (1961).
- ¹⁴T. Sebe, F. Khanna, and M. Harvey, Nucl. Phys. A130, 342 (1969).
- ¹⁵John Philpott, private communication.
- ¹⁶D. H. Gloeckner and R. D. Lawson, Phys. Lett 53B, 313 (1974).
- ¹⁷F. Ajzenberg-Selove, Nucl. Phys. A281, 1 (1977).
- ¹⁸F. Iachello, private communication.
- ¹⁹W. L. Wang and C. M. Shakin, Phys. Rev. C 5 1898 (1972).
- ²⁰The extended boson approximation in this paper was called the hybrid boson approximation in F. Darema-Roger's Ph.D. thesis.
- ²¹F. Iachello and A. Arima, Phys. Lett. 53B, 309 (1974); 57B, 39 (1975).
- ²²A. Arima and F. Iachello, Ann. Phys. 99, 253 (1976); Kernfysisch Versneller Instituut, University of Groningen, Netherlands, report, 1977 (unpublished).